Candidate ionotropic taste receptors in the *Drosophila* larva

Shannon Stewart, Tong-Wey Koh, Arpan C. Ghosh, and John R. Carlson[1]

Department of Molecular, Cellular, and Developmental Biology, Yale University, New Haven, CT 06511

We examine in *Drosophila* a group of ~35 ionotropic receptors (IRs), the IR20a clade, about which remarkably little is known. Of 28 genes analyzed, *GAL4* drivers representing 11 showed expression in the larva. Eight drivers labeled neurons of the pharynx, a taste organ, and three labeled neurons of the body wall that may be chemosensory. Expression was not observed in neurons of one taste organ, the terminal organ, although these neurons express many drivers of the *Gr* (*Gustatory receptor*) family. For most drivers of the *IR20a* clade, we observed expression in a single pair of cells in the animal, with limited coexpression, and only a fraction of pharyngeal neurons are labeled. The organization of *IR20a* clade expression thus appears different from the organization of the *Gr* family or the *Odor receptor* (*Or*) family in the larva. A remarkable feature of the larval pharynx is that some of its organs are incorporated into the adult pharynx, and several drivers of this clade are expressed in the pharynx of both larvae and adults. Different IR drivers show different developmental dynamics across the larval stages, either increasing or decreasing. Among neurons expressing drivers in the pharynx, two projection patterns can be distinguished in the CNS. Neurons exhibiting these two kinds of projection patterns may activate different circuits, possibly signaling the presence of cues with different valence. Taken together, the simplest interpretation of our results is that the *IR20a* clade encodes a class of larval taste receptors.

taste | ionotropic receptors | taste receptors | larva

Olfaction and taste are mediated by receptors of widely diverse families (1, 2). Studies of receptor expression have been critical to our understanding of chemosensory perception. Historically, the identification of several classes of receptors has been based largely on their expression patterns, with functional validation not becoming available until years later. Studies of receptor expression have informed our understanding of the principles of chemosensory coding. In some cases, analysis of receptor expression has suggested, and subsequently revealed, complex and elegant mechanisms of receptor gene regulation. Finally, in many cases, elucidation of receptor expression patterns has allowed chemosensory stimuli of particular ecological, evolutionary, or behavioral significance to be assigned to individual receptors.

The *Drosophila* larva offers major advantages as an organism in which to study the molecular and cellular basis of taste. The larval taste system is relatively simple and can be investigated with incisive molecular and genetic approaches. Understanding the molecular and cellular mechanisms by which *Drosophila* larvae evaluate potential food sources may suggest means of manipulating the feeding of other insect larvae, some of which consume agricultural crops and collectively cause immense damage to the world's agricultural output (3).

The head of the *Drosophila* larva contains three external chemosensory organs (4) (Fig. 1). The dorsal organ (DO) is innervated by the dendrites of 21 olfactory neurons and nine gustatory neurons. The terminal organ (TO) and ventral organ contain the dendrites of ~21 and approximately seven gustatory neurons, respectively.

There are also internal chemosensory organs lining the pharynx, each existing as a bilaterally symmetrical pair: the dorsal, ventral,

and posterior pharyngeal sensilla (DPS, VPS, and PPS, respectively) (5–7) (Fig. 1). Each organ contains ~17, 16, and 6 neurons, respectively, most of which are likely to be gustatory (5). Another organ, the dorsal pharyngeal organ (DPO), contains five neurons (3, 5, 8). A variety of other neurons in the body wall of the thorax and abdomen, and at the posterior tip of the larva, are also likely to be chemosensory (9–11).

The *Gustatory receptor* (*Gr*) family comprises 60 genes (12, 13). Expression analysis of the *Gr* genes using the *GAL4-UAS* system has shown that 39 of the predicted proteins are likely to be expressed in the TO, DPS, VPS, or PPS of the larva (11, 14, 15). However, a receptor-to-neuron map of the TO neurons suggested that many TO neurons did not express any *Gr* genes, consistent with the notion that some larval taste neurons may express other kinds of taste receptors (15).

The *Ionotropic receptor* (*IR*) family comprises 60 genes, of which members of one clade encode odor receptors (16). Another clade of 35 *IR* genes, called the *IR20a* clade, was recently shown to be expressed in gustatory neurons of *Drosophila* adults (17). Analysis of *GAL4* drivers of 28 genes of the clade revealed expression of 16 drivers in adult taste neurons, collectively representing all taste organs of the fly. Virtually nothing is known of their expression in larvae.

Here, we carry out a systematic expression analysis of the *IR20a* clade in the larval gustatory system. We find that 11 of the *GAL4* drivers show expression in larval gustatory organs. Seven drivers are expressed in the DPS, with different drivers expressing in different DPS neurons, and one of these drivers is also expressed in the VPS. Another driver is expressed in the DPO; another is expressed in nonneuronal cells of the TO; and three are expressed in the body wall, where they are associated with sensory hairs, sensory cones, and trachea. The neurons that

---

Significance

The coding of taste is based on the activity of taste receptors. We examine in *Drosophila* the expression of a group of ~35 ionotropic receptors (IRs), the IR20a clade, about which remarkably little is known. We find evidence that 11 are expressed in the larva. Most are expressed in neurons of the pharynx, a taste organ. Others are expressed in body-wall neurons that may be chemosensory. The organization of *IR* gene expression differs from the organization of expression of *Gustatory receptor* taste receptor genes. Among neurons expressing IR20a receptors in the pharynx, two projection patterns in the CNS can be distinguished, perhaps representing cues with different valence. Our results suggest that the IR20a clade encodes a class of larval taste receptors.
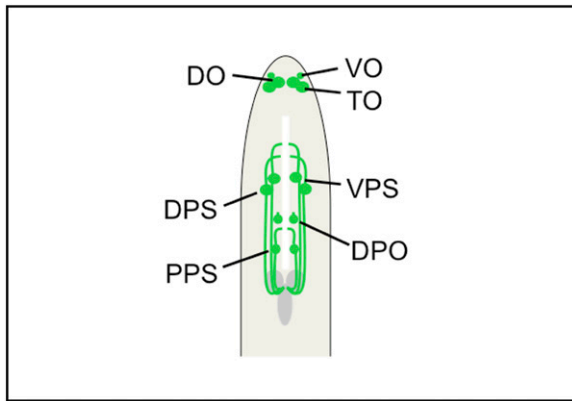
Fig. 1. Chemosensory organs in the larval head and pharynx. VO, ventral organ. We have depicted the VPS as anterior to the DPS, but they are close and their apparent relative positions depend on the viewing angle. The DPO is more difficult to identify than the other organs, and its position relative to the DPS and PPS may depend on the larval stage; we have not depicted neural processes for it.

express the drivers show different projection patterns in the larval CNS. Some drivers show dynamic expression patterns over the course of development. The simplest interpretation of the results is that the *IR20a* clade encodes a class of larval taste receptors.

Results

We examined 122 *GAL4* lines representing 28 members of the *IR20a* clade of *IR* genes. Thus, on average, four independent lines were examined for each gene. The *IR-GAL4* drivers were those drivers constructed and used by Koh et al. (17). In most cases, the *GAL4* gene was flanked by both 5′ and 3′ regions of the *IR* genes in an effort to maximize fidelity of the reporter. Most transgenes were integrated at common positions using the *phiC31* system to minimize genomic position effects (18–22). Expression was assessed using a membrane-bound GFP encoded by *UAS-mCD8-GFP* (23).

Each line was screened by examining first-, second-, and third-instar larvae. For each *IR* gene that showed GFP labeling at any stage, we chose one line that was representative, as judged by an analysis of the numbers of labeled cells. For most genes, however, the lines were very similar, and any of several lines could have been chosen as representative. We note that although first-instar larvae were viewed in their entirety, second- and third-instar larvae were dissected and the midgut and hindgut were removed to reduce autofluorescence from the gut or its contents. It is thus possible that one or more *GAL4* constructs drive expression in intestinal cells not examined in this screen.

Taste Organs of the Larval Head Express Nine *IR20a*-Clade Drivers, Some in Dynamic Patterns. A total of nine drivers of the *IR20a* clade showed expression in taste organs of the larval head. Drivers corresponding to seven genes (*IR48c, IR60b, IR60e, IR67b, IR67c, IR94f,* and *IR94h*) were expressed in the DPS (Fig. 2; an additional set of images showing the location of labeling with respect to the head skeleton is illustrated in Fig. S1; also discussed below). The patterns were remarkable in their sparseness of expression: In most cases, a single, bilaterally symmetrical pair of neurons was observed in the first-instar larva, although *IR67c-GAL4* showed some additional expression in the CNS. The *IR20a-GAL4* driver labeled a pair of neurons too, but they are located in the DPO (Fig. 2; also discussed below).

Third-instar larvae showed similar expression patterns for the seven DPS drivers, with some exceptions (Fig. 3). Drivers representing *IR60b, IR60e, IR67b, IR67c,* and *IR94f* also show

labeling of a single neuron in each of the bilaterally symmetrical DPS organs in early and middle third-instar larvae, as in the first instar. However, *IR48c-GAL4* drove little if any expression in the third instar, unlike in the first instar. We also that little if any labeling of *IR67b-GAL4* was observed in the late third instar. Thus, in these cases, labeling decreases over developmental time. *IR94h-GAL4* drove expression in the DPS, as in the first instar, but usually in two bilaterally symmetrical pairs of neurons rather than one pair (Fig. 3*F*). Thus, in this case, increased labeling was observed over developmental time. *IR20a-GAL4* drove expression in the DPO, as in the first instar (a lateral view is shown in Fig. 3 *G* and *H*).
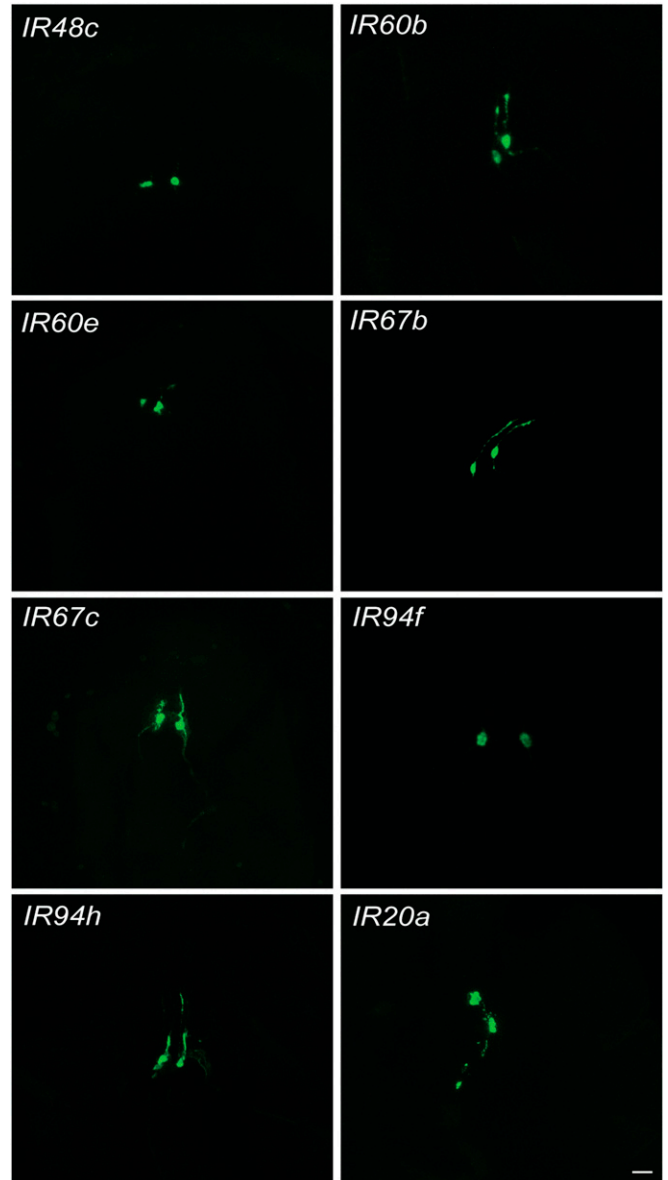
Fig. 2. Expression in the first instar. Drivers of *IR48c, IR60b, IR60e, IR67b, IR67c, IR94f,* and *IR94h* are expressed in a single bilaterally symmetrical pair of neurons in the DPS. Expression of *IR60b-GAL4* is weak. In the case of some drivers, such as *IR67b-GAL4*, dendrites can be seen to extend in the anterior direction from the cell bodies. The neurons that express the *IR20a* driver have shorter anterior projections and appear to be located in the DPO. Anterior is located at the top of the panels. (Scale bar: 20 μM.) An additional set of images showing the localization of labeling with respect to the head skeleton is shown in Fig. S1.

IR60b-GAL4 provides another example of dynamics in expression pattern. In addition to the pair of DPS neurons seen in the first and third instars (Figs. 2 and 3*A*), during the second instar, a second pair of labeled neurons can be seen in the VPS (Fig. 3 *I* and *J*).

Our identification of the labeled organs as the DPS, VPS, and DPO was based initially on the position of the labeled cells with respect to the head skeleton (Figs. 2 and 3 *H, J,* and *L* and Fig. S1). As a further test of this identification, we carried out systematic double labeling with the drivers and an anti-IR25a antibody. IR25a is a highly conserved IR that has previously been shown to label larval pharyngeal organs and may act as a coreceptor with other IRs (24, 25). An example of this double labeling is shown in Fig. 3 *K* and *L*, and double labeling for all drivers is shown in Fig. S2. Additional images of the colabeling at high magnification, from an independent experiment, are provided in Fig. 4. All drivers label cells that are either IR25a$^+$ or in very close proximity to IR25a$^+$ cells. The identification of the IR25a$^+$ pharyngeal organs as sensory organs is consistent with the results of a double-label experiment with the anti-IR25a antibody and an anti-Elav antibody (Fig. S2 *A, 3*). Although a definitive conclusion is precluded by the fact that neither anti-IR25a nor anti-Elav antibodies are specific for pharyngeal organs, the simplest interpretation of all of the data taken together is that the organs labeled by the drivers are the DPS, VPS, and DPO.

The TO was labeled by *IR47a-GAL4* (Fig. S3 *A* and *B*). We carried out a double-label experiment with a marker for the closely associated DO, *Orco-RFP*, which labels olfactory receptor neurons (Fig. S3 *C–E*). The merged image confirms the identification of the structure labeled by *IR47a-GAL4* as the TO, but the labeling pattern appears distinct from the labeling pattern expected of chemosensory neurons. A double-label experiment with a pan-neuronal nuclear marker, anti-Elav, does not reveal coexpression (Fig. S3 *F–H*). It thus seems likely that *IR47a-GAL4* labels nonneuronal support cells of the TO, but further analysis will be required to identify the labeled cell types definitively; interestingly, in the adult taste system, *IR47a-GAL4* expression appears to be neuronal (17). We note that nonneuronal expression has also been found for a member of the DEG/EnaC family of channels in the adult taste system (26).

In addition to examining these drivers of the IR20a clade, we examined three GAL4 drivers of another clade of the IR superfamily: *IR76b-GAL4, IR25a-GAL4,* and *IR8a-GAL4* (16, 24). IR76b has been shown to form heteromultimers with antennal IRs (25). It is also expressed in gustatory sensilla of the adult fly and has been found to be required for attraction to low concentrations of salt (27). We found that an *IR76b-GAL4* driver labels the DPS, VPS, DPO, and PPS, as well as the TO and the DO (Fig. S4), consistent with the possibility that IR76b forms heteromultimers with members of the IR20a clade.

IR25a-GAL4 labels larval taste organs, including the DPS, VPS, DPO, PPS, and TO, as well as the DO (Fig. S4); these results are consistent with the labeling of larval pharyngeal organs with anti-IR25 antibody (24) (Figs. 3 *K* and *L* and 4 and Fig. S2). By contrast, we did not observe expression of an *IR8a-GAL4* driver in taste organs of the larval head, although it is expressed broadly in the adult olfactory system (25).

Fig. 3. Expression in later instars. (*A–F*) Expression in the third-instar DPS, dorsal view. Anterior is located at the top of the panels. In *A*, the arrowhead indicates a dendrite and the arrow indicates the cell body. (Scale bar: 20 μM.) (*G*) *IR20a* driver expression in the third-instar DPO, lateral view. Anterior is located to the left of the panel. (*H*) Differential interference contrast (DIC) image of *G*, showing positions of labeled cells relative to the mouth hooks (dark). (Scale bar: 10 μM.) (*I*) Transient *IR60b* driver expression in the VPS (arrowhead) during the second instar, lateral view. The arrow indicates expression in the DPS. Anterior is located to the left of the panel. (*J*) DIC image of *I*. (Scale bar: 10 μM.) (*K*) Double labeling of *IR67c-GAL4* and IR25a visualized with an anti-IR25a antibody, dorsal view. (*L*) Double labeling of *IR67c-GAL4* and IR25a, DIC image, seen in a lateral view. The arrow indicates the DPS, showing colabeling, and the arrowhead indicates the VPS, which is labeled only by anti-IR25a antibody.
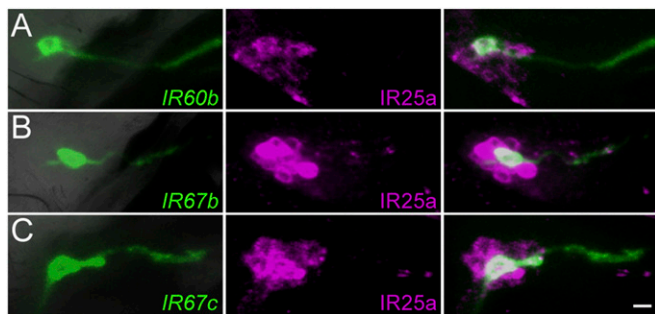
Fig. 4. Pharyngeal taste neurons double-labeled with anti-IR25a antibody (magenta) and GAL4 drivers (GFP, green) of *IR60b* (*A*), *IR67b* (*B*), and *IR67c* (*C*). The images are presented in lateral views. (*Left*) GFP fluorescence superimposed on DIC images. (*Center*) Anti-*IR25a* labeling and (*Right*) GFP fluorescence superimposed on anti-*IR25a* labeling. (Scale bar: 5 μm.)

Expression of *IR20a* Clade Drivers in the Body. In addition to its expression in the DPS, *IR67b-GAL4* is expressed in the body. Labeling is observed in cells of the abdominal segments, which could function in contact chemosensation, or perhaps in another sensory modality (Fig. 5 *A–C*).

IR56a-GAL4 is expressed in a small subset of neurons in segments six and seven of the abdomen, with expression observed somewhat less consistently in segment five (Fig. 5 *D* and *E*). Interestingly, neurons labeled by *IR56a-GAL4* are often observed closely associated with the trachea, which transport gases to and from tissues (arrowhead in Fig. 5*E*). The labeled neurons often appear to contain two dendritic projections and an axon that projects toward the ventral nerve cord of the CNS. Expression is also observed in neurons whose cell bodies are located in the posterior portion of the ventral nerve cord (Fig. S5). We note that the endogenous *IR56a* gene is located in the intron of the *serotonin receptor 1A* gene, which is expressed in the larval CNS (28).

IR94d-GAL4 expression is observed at the posterior end of the abdomen in neurons that send dendrites into sensory cones (Fig. 5*F*). These neurons may have a chemosensory role in sensing local gas concentrations and in mediating an escape behavior that is triggered by hypoxia or hyperoxia (9, 29); more detailed analysis will be required to determine their functional identity. Labeling was occasionally observed in the body wall of other abdominal segments. We note that although the great majority of drivers examined in this analysis contained both 5′ and 3′ flanking regions from each endogenous *IR* gene, the abdominal staining was observed with an *IR94d-GAL4* driver that contained only 5′ sequences. *IR25a-GAL4* also labels neurons that innervate sensory cones on the posterior portion of the abdomen, reminiscent of the pattern of *IR94d-GAL4*, as well as other cells in the thorax and abdomen.

Expression of *IR20a* Clade Drivers Is Distributed Among Multiple Pharyngeal Neurons. Having established that seven drivers of the *IR20a* clade each label one pair of neurons in the DPS, we wondered whether they were all coexpressed in the same pair. To address this question, we crossed pairs of drivers and asked whether the resulting expression patterns were additive or overlapping in heterozygous animals (Fig. 6). When we crossed *IR60e-GAL4* and *IR67c-GAL4*, each of which labeled DPS neurons in the third instar, the heterozygous offspring showed two pairs of labeled DPS neurons. The simplest interpretation of these results is that the two drivers label different pairs of DPS neurons. Similar crosses revealed that *IR60e-GAL4* is expressed in different DPS neurons from *IR94f-GAL4* and that *IR67c-GAL4* is expressed in different DPS neurons from *IR94f-GAL4*. The simplest interpretation of these results is that there are at least three

distinguishable classes of DPS neurons in the third instar, each expressing a different member of the *IR20a* clade.

Projections of Neurons to the Subesophageal Ganglion. The primary taste center of the larval brain is the subesophageal ganglion (SOG) (14, 15, 30). Different *IR-GAL4* lines exhibit different projection patterns within the SOG (Fig. 7). Drivers of *IR60e*, *IR67c*, and *IR94h*, which express in the DPS, label projections that extend to, or very near to, the midline. By contrast, drivers of *IR67b* and *IR94f* also express in the DPS but extend projections that appear distinct from the projections of *IR60e*, *IR67c*, and *IR94h*. The patterns of these five lines are reminiscent of patterns observed for certain *Gr-GAL4* drivers that are expressed in the DPS (15). Projections in the SOG were not detected for *IR20a-GAL4*, which is expressed in the DPO, or for *IR94d-GAL4*, which is expressed in the abdomen, nor did we observe projections for *IR48c-GAL4*, which was examined in the small SOG of the first instar, or *IR60b-GAL4*, which is a weak driver. We did not observe projections in the CNS for *IR47a-GAL4*–expressing cells, consistent with the data indicating they are nonneuronal.

Discussion

We have shown that the *IR20a* clade is likely to encode a class of larval taste receptors. There have been virtually no previous data on the expression of these genes in the larva.
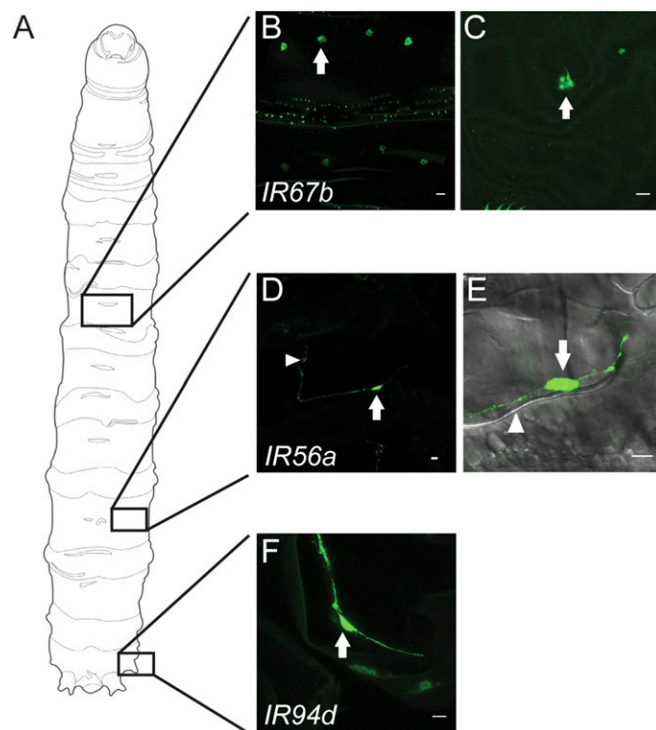
Fig. 5. Expression in the body. (*A*) Schematic of the larval third-instar body viewed from the ventral side. Modified with permission from ref. 43. (*B*) *IR67b-GAL4* expression on the ventral surface. The arrow indicates driver expression. Puncta are autofluorescent denticle belts. (Scale bar: 20 μm.) (*C*) High-magnification view of a bifurcated sensillum surrounded by cells expressing *Ir67b-GAL4*. The arrow indicates driver expression. (Scale bar: 10 μm.) (*D*) Expression of *IR56a-GAL4* in lateral bidendritic neurons in abdominal segments 5, 6, and 7. The white arrow indicates the cell body, and the arrowhead indicates the neuronal process. (Scale bar: 10 μm.) (*E*) Cell expressing *IR56a-GAL4*. The white arrow indicates the cell body, and the white arrowhead indicates an unlabeled tracheum. (Scale bar: 10 μm.) (*F*) *IR94d-GAL4* expression in a neuron that sends a dendrite into a sensory cone. The white arrow indicates the cell body. (Scale bar: 10 μm.)
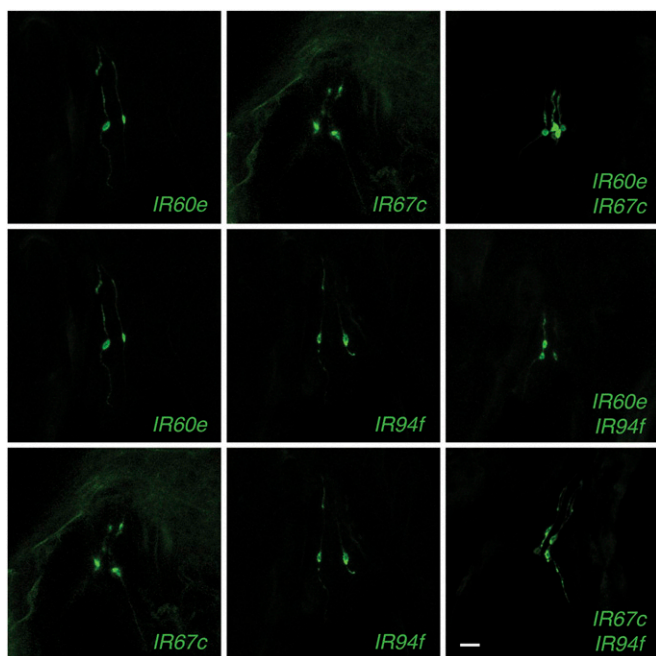
Fig. 6. Combinatorial analysis of drivers in third instar. At the top, *IR60e-GAL4* and *IR67c-GAL4* are each expressed in a single pair of cells in the pharynx; in the double-driver combination, four cell bodies are visible, indicating that the patterns are additive. The other combinations are also additive, although in the case of the combination of *IR60e-GAL4* and *IR94f-GAL4*, one cell body is out of the plane of focus. (Scale bar: 20 μm.)

Organization of Expression. We have analyzed the expression of the IR20a clade using *GAL4* drivers. To maximize the reliability of our analysis, we have (*i*) used drivers that contain not only sequences 5′ to the *IR* genes but sequences 3′ to the *IR* genes as well, (*ii*) inserted most drivers into common positions in the genome via the *φC31* system, and (*iii*) examined multiple insertions of almost all constructs. Efforts to confirm expression patterns by in situ hybridization were made for some genes using a variety of methods, including tyramide signal amplification, but were unsuccessful, presumably due to low expression levels (16, 17).

Of 28 members of this clade, drivers representing 11 showed expression in the larva. Eight of these drivers labeled the pharynx, and three drove expression in neurons of the body wall that may transmit chemical information. Within the pharynx, we observed expression in the DPS, the VPS, and the DPO, but not in the PPS. Surprisingly, we did not observe expression in neurons of the TO, although these neurons collectively express 27 drivers of the *Gr* family. By contrast, *Gr* expression has not been reported in the DPO.

One interpretation of the expression of *IR20a* genes in the pharynx, but not the TO, is that these IRs recognize metabolites that are produced by digestion in the anterior portion of the gastrointestinal tract. Many compounds in the larval environment may contain sugar, acetyl, methyl, or other groups that are removed during digestion. Perhaps some IRs in the pharynx recognize certain key molecules only after they have been unmasked in transit toward the pharynx. Another possibility is that IRs and Grs have different dynamic ranges (e.g., they recognize the same tastants but with different sensitivities), possibly reflecting different roles in reflexive behaviors vs. gustatory learning (31–33).

Expression of the *IR20a* clade drivers is strikingly sparse. For most drivers, we observed expression in a single pair of cells in the animal. Double-driver analysis revealed that three drivers were expressed in different pairs of neurons in the DPS. Given that there are ~17 neurons in this organ (5), and seven drivers

expressed in the DPS, it is evident that only a fraction of DPS neurons express drivers of the *IR20a* clade.

Of a collection of *GAL4* drivers representing all 68 members of the *Gr* family of taste receptors, 19 showed expression in the DPS, with each of these drivers showing expression in one or two pairs of DPS neurons. It will be interesting to determine how Gr expression and IR expression are coordinated in the DPS (i.e., how many cells express only Grs, how many express only IRs, how many express both).

The organization of *IR20a* clade expression appears different from the organization of expression of the *Odor receptor* (*Or*) family or the *Gr* family in the larva. *Or* genes are collectively expressed in all or nearly all of the olfactory receptor neurons in the larval olfactory organ, in most cases in a one receptor/one neuron fashion. *Gr* drivers, by contrast, are expressed in only a fraction of cells of the larval taste organs (15) and are coexpressed, in some cases, at high multiplicity: Within the TO ganglion, 17 *Gr-GAL4* drivers are coexpressed in the C1 cell and seven drivers are coexpressed in the C2 cell (15). Moreover, many *Gr* genes are expressed in more than one pair of cells in the larval gustatory system. Expression of the *IR20a*-clade drivers displays a third pattern of organization. Unlike the *Or* genes, expression appears to be restricted to a limited subset of cells in the organs in which they are expressed. Unlike the *Gr* genes, there appears to be relatively little coexpression, and few *IR20a* drivers are expressed in more than one pair of taste neurons.

A corollary of our present results, taken together with the results of a study by Kwon et al. (15), is that there remain many orphan neurons in the larval taste organs (i.e., neurons to which no receptor has been mapped). It will be interesting to determine how many of these cells express other classes of chemosensory receptors, such as members of the *pickpocket* (*ppk*) family of DEG/ENaC channels (34, 35) or *Transient receptor potential* (*Trp*) gene families (36), and how many of these cells serve other sensory modalities or perhaps other functions.

Development. A remarkable feature of the larval pharynx is that some of its organs are incorporated into the adult pharynx. Whereas most larval sense organs disintegrate and are replaced by adult organs deriving from imaginal discs, the DPS and PPS survive (5). The DPS splits and is remodelled into the ventral cibarial sense organ and the labral sense organ (LSO) of the adult pharynx. Consistent with this developmental persistence,
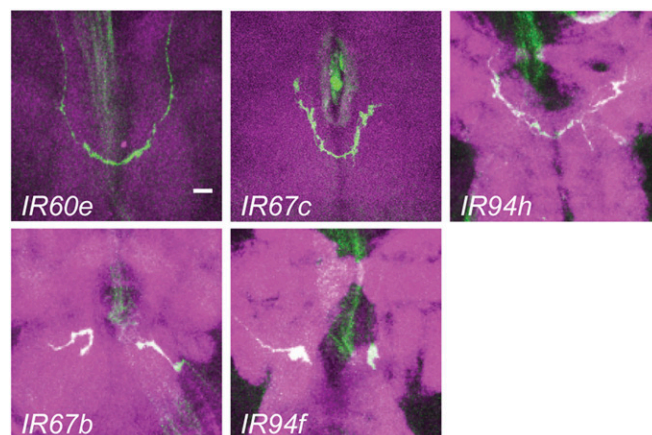
Fig. 7. Projection patterns in the SOG of the brain. Consistent with their circumscribed expression patterns, these drivers label a single pair of projections. Projections from neurons that express the *IR60e*, *IR67c*, and *IR94h* drivers approach or cross the midline, whereas projections from cells that express the *IR67b* and *IR94f* drivers do not. (Scale bar: 20 μm.)

drivers of *IR60b*, *IR67c*, *IR94f*, and *IR94h* are expressed in both the larval DPS (Fig. 3) and the adult LSO (17).

Two drivers, *IR48c-GAL4* and *IR67b-GAL4*, are expressed in the DPS in the first instar, but their expression appears to decline during the course of larval development. Consistent with this decline, expression of neither is observed in the adult pharynx. Not all drivers showed such a decline; in fact, *IR94h-GAL4* showed increasing expression, in the sense that expression is observed in one pair of neurons in the first instar but in two pairs in the third instar. We acknowledge that changes in GFP fluorescence may not represent the dynamics of IR protein changes precisely. Nonetheless, it seems clear that different drivers show different patterns of developmental dynamics.

Why might the profile of *IR* gene expression in the pharynx change during the course of larval development? One possibility is that patterns of gene expression change to accommodate different chemosensory needs. Although young larvae forage on the surface of the culture medium, they subsequently begin to exhibit a digging behavior and descend into the medium, where they may encounter different populations of microbiota and different chemical cues (37). Moreover, later in the third instar, larvae stop feeding and begin to search for a pupariation site. During this transition, new cues may become salient and some cues may even acquire a different valence. These changes may be reflected by changes in the patterns of IR expression. Some IRs may activate circuits that promote feeding, whereas others may activate circuits that promote the termination of feeding or migration from a food source to a pupariation site. Interestingly, such differing dynamics have not been previously documented for drivers of *Or* and *Gr* genes, to our knowledge.

Of 16 genes of the *IR20a* clade that are expressed in the adult (17), seven are expressed in larvae. Examples of drivers expressed in adults but not in larvae include *IR52c-GAL4* and *IR52d-GAL4*, which are coexpressed in cells of the male foreleg. These two genes have been implicated in sexual behaviors that are specific to adults, consistent with the adult-specific expression of these drivers. By contrast, some *IR* drivers, such as *IR67b-GAL4*, appear to be expressed in larvae but not adults.

Function. The expression patterns described here suggest avenues for exploration of function. *IR56a-GAL4*–expressing cells in the body wall resemble cells that act in the generation of rhythmic locomotion behavior (38, 39). It will be interesting to determine whether mutation of *IR56a* affects motor behavior. Likewise, the *IR94d-GAL4* expression pattern resembles the expression pattern of oxygen-sensing cells that function in an escape response elicited by hypoxia (9).

Among drivers that are expressed in the DPS, two projection patterns can be distinguished in the SOG. Neurons expressing drivers of *IR60e*, *IR67c*, and *IR94h* send projections to the midline; neurons expressing drivers of *IR67b* and *IR94f* do not reach the midline. The two classes of neurons may activate different circuits; one possibility among others is that they signal the presence of cues with distinct valence, such as aversive vs. appetitive (40). For several drivers, we did not observe projections in the SOG; a more sensitive and detailed analysis will be required to investigate the possibility that some of these other pharyngeal neurons drive other circuits.

Among 26 members of the *IR20a* clade analyzed, one gene, *IR60b*, is distinguished from all others by its rate of evolutionary change (17). Specifically, it exhibits a negative direction of selection value of −0.28 ($P = 0.004$), as measured by the McDonald–Kreitman test (41, 42). This value suggests evolutionary pressure to conserve the amino acid sequence of IR60b. One interpretation is that the structure of IR60b represents a successful solution to a difficult problem; perhaps it accurately evaluates the level of a critical cue that must not be mistaken for another cue.

Conclusion

In summary, we have shown that a class of IRs is expressed in neurons of the larval taste system. This study lays a foundation for detailed analysis of these receptors, the neurons in which they are expressed, and the circuits that they drive. It will be of special interest to determine how the expression and function of these receptors are integrated with the expression and function of the Grs in providing a molecular and cellular basis for the sense of taste.

Materials and Methods

Drosophila Stocks. All stocks were maintained on standard *Drosophila* cornmeal agarose media at 22 ± 2 °C. Animals reared for imaging were maintained at 25 °C beginning at egg laying. The reporter construct was *UAS-mCD8::GFP* (23).

Expression Constructs. Expression constructs are the same as those expression constructs described by Koh et al. (17). Briefly, 27 constructs bearing both the 5′ and 3′ flanking regions and three constructs containing only the 5′ flanking region were generated. When integrating the constructs with P elements, at least five and at most 10 independent lines were generated.

Table 1. Expression of drivers in taste organs

Driver	TO	DPS	VPS	DPO	Body	No. of lines examined
IR20a	−	−	−	+	−	7
IR47a	+	−	−	−	−	6
IR48b	−	−	−	−	−	2
IR48c	−	+*	−	−	−	6
IR51b	−	−	−	−	−	5
IR52a	−	−	−	−	−	7
IR52c	−	−	−	−	−	4
IR52d	−	−	−	−	−	2
IR54a	−	−	−	−	−	8
IR56a	−	−	−	−	+	7[†]
IR56b	−	−	−	−	−	2
IR56c	−	−	−	−	−	2
IR56d	−	−	−	−	−	6
IR60b	−	+	+[‡]	−	−	2
IR60d	−	−	−	−	−	2
IR60e	−	+	−	−	−	5[§]
IR62a	−	−	−	−	−	2
IR67a	−	−	−	−	−	7
IR67b	−	+[¶]	−	−	+	4
IR67c	−	+	−	−	−	9
IR94a	−	−	−	−	−	3
IR94b	−	−	−	−	−	1
IR94c	−	−	−	−	−	6
IR94d	−	−	−	−	+	7
IR94e	−	−	−	−	−	4
IR94f	−	+	−	−	−	2
IR94g	−	−	−	−	−	2
IR94h	−	+[#]	−	−	−	2

IR60b drivers showed lower expressivity and penetrance than the other drivers. *IR94d-GAL4* showed a higher variability of expression pattern than the other drivers. As indicated in the main text, patterns are not identical at all times in development for all drivers (e.g., *IR60b-GAL4* showed expression in the VPS during the second instar but not early or late in larval development).
*Little if any labeling was observed in the third instar.
[†]Different lines of this driver showed marked variation in the number of labeled segments and in the overall intensity of labeling.
[‡]Labeling was observed in the second-instar VPS.
[§]One line showed expression in an additional pair of cells lateral to the head skeleton, in addition to labeling in the DPS.
[¶]Little if any labeling was observed in the late third instar.
[#]One pair of cells was labeled in the first-instar DPS; additional cells were labeled in the third-instar DPS.

When integrating using the ϕC31 method (20), at least two lines were generated with constructs at defined integration sites. We note that *IR60e* contains a small deletion at its C terminus; we do not know if this deletion affects its function or whether other alleles are present in wild populations.

Immunohistochemistry and Imaging. Larvae were reared at 25 °C before imaging. In most cases, animals were homozygous for both the *IR-GAL4* and *UAS-mCD8::GFP* constructs. For each *IR* gene examined, at least one line was examined in the doubly homozygous condition. We examined at least five independent lines for those constructs that were inserted with P elements and at least two lines for those constructs inserted using ϕC31 insertion sites, in all cases except *IR94b-GAL4* (Table 1).

For the initial survey of expression, at least 11 second- and third-instar *Drosophila* larvae were dissected in PBS; at least 25 first-instar larvae were screened subsequently. In the case of second- and third-instar larvae, a variety of dissection strategies were used to ensure the greatest coverage of organs and tissues, and an effort was made to preserve sensory cells of the head and body. In general, the midgut and hindgut were removed for imaging of second- and third-instar larvae because the gut or the food within is autofluorescent. Dissections were limited to ~15 min or less in duration. After dissection, animals were soaked for ~30 min in Vectashield mounting media (Vector Laboratories), mounted, and viewed on a Zeiss confocal microscope. First-instar larvae were collected on an apple juice agar egg-lay plate and flash-frozen ~24 h after egg laying. They were then carefully thawed and mounted whole. After thawing, and in some cases dissection,

animals were mounted in Vectashield mounting media and viewed on a Zeiss confocal microscope.

Immunohistochemistry protocols used in Figs. 4 and 7 and Fig. S3 *F–H* were based on a previously published technique (5). Samples of CNS tissue or larval heads were dissected, permeabilized, and fixed in a solution of PBS plus 0.4% Triton-X (PBS-T) and 3.7% (vol/vol) formaldehyde for at least 1 h. They were washed three times for at least 20 min each time in PBS. (In the case of head staining, the wash solution was PBS-T to increase permeability.) They were incubated for at least 1 h in PBS containing 1% normal goat serum. Primary antibodies were applied overnight at 4 °C with gentle shaking. Samples were subsequently washed and blocked, and secondary antibody was applied for at least 4 h at room temperature or overnight at 4 °C. For Fig. 7 and Fig. S3 *F–H*, rabbit anti-GFP antibodies were obtained from Invitrogen (1:500). Mouse anti-Elav concentrate (1:250) and mouse anti-nc82 (anti-Bruchpilot, 1:10) antibodies were obtained from the Developmental Studies Hybridoma Bank at the University of Iowa; secondary immunohistochemistry fluorophores, goat anti-rabbit 488, and goat anti-mouse 568 were obtained from Invitrogen (1:500). Antibody concentrations used in Fig. 4, including the anti-IR25a antibody (a gift from Richard Benton, University of Lausanne, Lausanne, Switzerland), are provided in *SI Materials and Methods*. The resulting images were processed using NIH ImageJ and Adobe Photoshop.

1. Su CY, Menuz K, Carlson JR (2009) Olfactory perception: Receptors, cells, and circuits. *Cell* 139(1):45–59.
2. Liman ER, Zhang YV, Montell C (2014) Peripheral coding of taste. *Neuron* 81:984–1000.
3. van der Goes van Naters W, Carlson JR (2006) Insects as chemosensors of humans and crops. *Nature* 444(7117):302–307.
4. Stocker RF (1994) The organization of the chemosensory system in Drosophila melanogaster: A review. *Cell Tissue Res* 275(1):3–26.
5. Gendre N, et al. (2004) Integration of complex larval chemosensory organs into the adult nervous system of Drosophila. *Development* 131(1):83–92.
6. Python F, Stocker RF (2002) Adult-like complexity of the larval antennal lobe of D. melanogaster despite markedly low numbers of odorant receptor neurons. *J Comp Neurol* 445(4):374–387.
7. Singh RN, Singh K (1984) Fine structure of the sensory organs of Drosophila melanogaster Meigen larva (Diptera: Drosophilidae). *Int J Insect Morphol Embryol* 13(4):255–273.
8. Campos-Ortega JA (1997) *The Embryonic Development of Drosophila Melanogaster* (Springer, Berlin).
9. Vermehren-Schmaedick A, Ainsley JA, Johnson WA, Davies SA, Morton DB (2010) Behavioral responses to hypoxia in Drosophila larvae are mediated by atypical soluble guanylyl cyclases. *Genetics* 186(1):183–196.
10. Grueber WB, et al. (2007) Projections of Drosophila multidendritic neurons in the central nervous system: Links with peripheral dendrite morphology. *Development* 134(1):55–64.
11. Thorne N, Amrein H (2008) Atypical expression of Drosophila gustatory receptor genes in sensory and central neurons. *J Comp Neurol* 506(4):548–568.
12. Clyne PJ, Warr CG, Carlson JR (2000) Candidate taste receptors in *Drosophila*. *Science* 287(5459):1830–1834.
13. Robertson HM, Warr CG, Carlson JR (2003) Molecular evolution of the insect chemoreceptor gene superfamily in Drosophila melanogaster. *Proc Natl Acad Sci USA* 100 (Suppl 2):14537–14542.
14. Colomb J, Grillenzoni N, Ramaekers A, Stocker RF (2007) Architecture of the primary taste center of Drosophila melanogaster larvae. *J Comp Neurol* 502(5):834–847.
15. Kwon JY, Dahanukar A, Weiss LA, Carlson JR (2011) Molecular and cellular organization of the taste system in the Drosophila larva. *J Neurosci* 31(43):15300–15309.
16. Benton R, Vannice KS, Gomez-Diaz C, Vosshall LB (2009) Variant ionotropic glutamate receptors as chemosensory receptors in *Drosophila*. *Cell* 136(1):149–162.
17. Koh TW, et al. (2014) The Drosophila IR20a clade of ionotropic receptors are candidate taste and pheromone receptors. *Neuron* 83(4):850–865.
18. Bischof J, Maeda RK, Hediger M, Karch F, Basler K (2007) An optimized transgenesis system for *Drosophila* using germ-line-specific phiC31 integrases. *Proc Natl Acad Sci USA* 104(9):3312–3317.
19. Fish MP, Groth AC, Calos MP, Nusse R (2007) Creating transgenic Drosophila by microinjecting the site-specific phiC31 integrase mRNA and a transgene-containing donor plasmid. *Nat Protoc* 2(10):2325–2331.
20. Groth AC, Fish M, Nusse R, Calos MP (2004) Construction of transgenic Drosophila by using the site-specific integrase from phage phiC31. *Genetics* 166(4):1775–1782.
21. Markstein M, Pitsouli C, Villalta C, Celniker SE, Perrimon N (2008) Exploiting position effects and the gypsy retrovirus insulator to engineer precisely expressed transgenes. *Nat Genet* 40(4):476–483.
22. Boy AL, et al. (2010) Vectors for efficient and high-throughput construction of fluorescent Drosophila reporters using the PhiC31 site-specific integration system. *Genesis* 48(7):452–456.
23. Lee T, Luo L (1999) Mosaic analysis with a repressible cell marker for studies of gene function in neuronal morphogenesis. *Neuron* 22(3):451–461.
24. Croset V, et al. (2010) Ancient protostome origin of chemosensory ionotropic glutamate receptors and the evolution of insect taste and olfaction. *PLoS Genet* 6(8):e1001064.
25. Abuin L, et al. (2011) Functional architecture of olfactory ionotropic glutamate receptors. *Neuron* 69(1):44–60.
26. Ben-Shahar Y, et al. (2010) The Drosophila gene CheB42a is a novel modifier of Deg/ENaC channel function. *PLoS ONE* 5(2):e9395.
27. Zhang YV, Ni J, Montell C (2013) The molecular basis for attractive salt-taste coding in Drosophila. *Science* 340(6138):1334–1338.
28. Luo J, Becnel J, Nichols CD, Nässel DR (2012) Insulin-producing cells in the brain of adult Drosophila are regulated by the serotonin 5-HT1A receptor. *Cell Mol Life Sci* 69(3):471–484.
29. Morton DB, Stewart JA, Langlais KK, Clemens-Grisham RA, Vermehren A (2008) Synaptic transmission in neurons that express the Drosophila atypical soluble guanylyl cyclases, Gyc-89Da and Gyc-89Db, is necessary for the successful completion of larval and adult ecdysis. *J Exp Biol* 211(Pt 10):1645–1656.
30. Vosshall LB, Stocker RF (2007) Molecular architecture of smell and taste in Drosophila. *Annu Rev Neurosci* 30:505–533.
31. El-Keredy A, Schleyer M, König C, Ekim A, Gerber B (2012) Behavioural analyses of quinine processing in choice, feeding and learning of larval Drosophila. *PLoS ONE* 7(7):e40525.
32. Niewalda T, et al. (2008) Salt processing in larval Drosophila: Choice, feeding, and learning shift from appetitive to aversive in a concentration-dependent way. *Chem Senses* 33(8):685–692.
33. Schipanski A, Yarali A, Niewalda T, Gerber B (2008) Behavioral analyses of sugar processing in choice, feeding, and learning in larval Drosophila. *Chem Senses* 33(6):563–573.
34. Liu L, Yermolaieva O, Johnson WA, Abboud FM, Welsh MJ (2003) Identification and function of thermosensory neurons in Drosophila larvae. *Nat Neurosci* 6(3):267–273.
35. Zelle KM, Lu B, Pyfrom SC, Ben-Shahar Y (2013) The genetic architecture of degenerin/epithelial sodium channels in Drosophila. *G3 (Bethesda)* 3(3):441–450.
36. Al-Anzi B, Tracey WD, Jr, Benzer S (2006) Response of Drosophila to wasabi is mediated by painless, the fly homolog of mammalian TRPA1/ANKTM1. *Curr Biol* 16(10):1034–1040.
37. Godoy-Herrera R (1986) The development and genetics of digging behaviour in Drosophila larvae. *Heredity* 56(1):33–41.
38. Hughes CL, Thomas JB (2007) A sensory feedback circuit coordinates muscle activity in Drosophila. *Mol Cell Neurosci* 35(2):383–396.
39. Song W, Onishi M, Jan LY, Jan YN (2007) Peripheral multidendritic sensory neurons are necessary for rhythmic locomotion behavior in Drosophila larvae. *Proc Natl Acad Sci USA* 104(12):5199–5204.
40. Mishra D, et al. (2013) The molecular basis of sugar sensing in Drosophila larvae. *Curr Biol* 23(15):1466–1471.
41. McDonald JH, Kreitman M (1991) Adaptive protein evolution at the Adh locus in Drosophila. *Nature* 351(6328):652–654.
42. Stoletzki N, Eyre-Walker A (2011) The positive correlation between dN/dS and dS in mammals is due to runs of adjacent substitutions. *Mol Biol Evol* 28(4):1371–1380.
43. Wipfler B, et al. (2013) The skeletomuscular system of the larva of Drosophila melanogaster (Drosophilidae, Diptera): A contribution to the morphology of a model organism. *Arthropod Struct Dev* 42(1):47–68.